

Article

Separation of the Glycosylated Carotenoid Myxoxanthophyll from *Synechocystis Salina* by HPCCC and Evaluation of Its Antioxidant, Tyrosinase Inhibitory and Immune-Stimulating Properties

Michaela Nováková^{1,2}, Tereza Fábryová^{1,2} , Doris Vokurková³, Iva Dolečková⁴, Jiří Kopecký¹, Pavel Hrouzek¹, Lenka Tůmová² and José Cheel^{1,*}

¹ Laboratory of Algal Biotechnology—Centre ALGATECH, Institute of Microbiology of the Czech Academy of Sciences, Opatovický Mlýn, 379 81 Třeboň, Czech Republic; novakova.m7@seznam.cz (M.N.); fabryova.tereza@gmail.com (T.F.); kopecky@alga.cz (J.K.); hrouzek@alga.cz (P.H.)

² Department of Pharmacognosy, Faculty of Pharmacy, Charles University, Akademika Heyrovského 1203, 500 05 Hradec Králové, Czech Republic; tumova@faf.cuni.cz

³ Institute of Clinical Immunology and Allergology, Faculty of Medicine and University Hospital, Charles University, Sokolská 581, 500 05 Hradec Králové, Czech Republic; vokurkovad@lfhk.cuni.cz

⁴ Contipro a.s., Dolní Dobrouč 401, 561 02 Dolní Dobrouč, Czech Republic; iva.doleckova@contipro.com

* Correspondence: jcheel@email.cz or jcheel@alga.cz; Tel.: +420-384-340-465

Received: 23 November 2020; Accepted: 10 December 2020; Published: 15 December 2020



Abstract: Global demand for natural pigments has increased in the past few years. Myxoxanthophyll, a glycosylated monocyclic carotenoid, is a pigment that occurs naturally in cyanobacteria but no scalable isolation process has been developed to obtain it from its natural source to date. In this study, myxoxanthophyll was isolated from unicellular cyanobacterium *Synechocystis salina* (*S. salina*) using high-performance countercurrent chromatography (HPCCC), where the lower phase of the biphasic solvent system composed of *n*-heptane–ethanol–water (2:4:4, *v/v/v*) was used as a mobile phase, whereas its upper phase was the stationary phase. For the HPCCC isolation, a multi-injection method was developed, and four consecutive sample injections (70 mg each) were performed, obtaining, in total, 20 mg of myxoxanthophyll, which was finally purified with high-performance liquid chromatography (HPLC). Overall, a final myxoxanthophyll yield of 15 mg (98% purity) was obtained. The target pigment showed a weak antioxidant and tyrosinase inhibitory effect, and exhibited immune-stimulating properties by activating human granulocytes. The results presented here form a basis for the large-scale production of myxoxanthophyll, and show the potential benefits of this pigment for human health.

Keywords: myxoxanthophyll; cyanobacteria; *Synechocystis*; high-performance countercurrent chromatography (HPCCC); countercurrent chromatography (CCC); centrifugal partition chromatography (CPC)

1. Introduction

Currently, the global market of carotenoid pigments is led by the products derived from organic synthesis; however, the growing evidence of the danger of consuming synthetic pigments has encouraged the consumers to prefer natural pigments in nutraceuticals, food and cosmetics. Cyanobacterium *Synechocystis* has been one of the most extensively studied species since it was initially isolated from a fresh lake in 1968 [1]. It was reported to biosynthesize different types of pigments including chlorophyll, carotenoids and phycobiliproteins, many of which have attracted the attention

of the industries and researchers due to their varied bio-functionality and applications [2]. One of the carotenoid pigments synthesized by *Synechocystis* is myxoxanthophyll (Figure 1), a glycosylated monocyclic carotenoid that is rarely found in nature [3,4]. This yellow pigment has been shown to exhibit antioxidant and anti-hyperglycemic activities [5,6]. The potential of myxoxanthophyll in the prophylactic and/or therapeutic treatment of undesirable conditions due to oxidative processes has also been disclosed [7]. To the best of our knowledge, this pigment has not yet been offered commercially, and its bio-functional properties of interest in the food, nutraceutical and cosmetic sectors have not been extensively addressed.

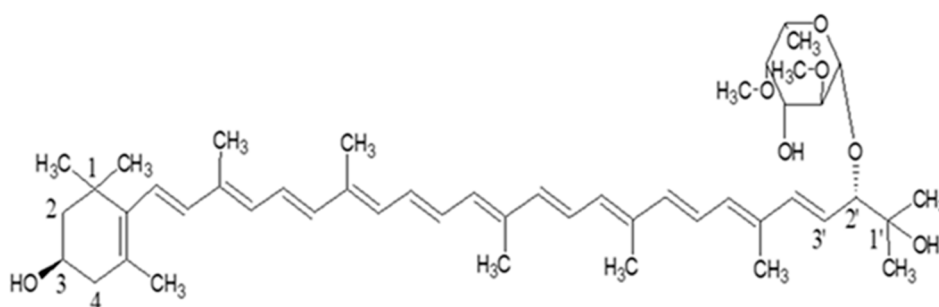


Figure 1. Chemical structure of myxoxanthophyll.

To date, myxoxanthophyll has been obtained from *Synechocystis* sp. biomass using multi-step procedures employing different solid-support columns [8], which required solvent- and time-consuming operations, thus making the whole process more complex and expensive. To make *Synechocystis*, a commercially exploitable source of myxoxanthophyll, the application of a scalable separation approach is needed. In this context, the use of high-performance countercurrent chromatography (HPCCC) technology might be relevant due to its high efficiency and proven scalability [9]. HPCCC lacks the need for any solid support, as two immiscible phases of a biphasic solvent system can be indistinctly used as a mobile or stationary phase [10]. The stationary phase is immobilized in the HPCCC column by means of a centrifugal force field generated by column spinning, whereas the mobile phase is pumped through the column. The HPCCC separation of target compounds from a mixture is based on the difference in their partitioning between two immiscible phases. Unlike solid-support chromatography, in HPCCC the liquid nature of the stationary phase gives this technique several advantages which include a large sample loading capacity, low risk of irreversible adsorption, high sample recovery, low consumption of solvents, and great operational versatility since the roles of the mobile and stationary phases can be exchanged during the chromatographic operation [10,11]. The efficiency of HPCCC in the purification of a wide variety of active compounds from natural sources has been extensively demonstrated [12–16] and its application at industrial level is already a reality [9]. The present study integrates the cultivation of *Synechocystis salina* (*S. salina*) and HPCCC technology to produce myxoxanthophyll, which was subsequently tested for its antioxidant, tyrosinase inhibitory, and immune-stimulating effects.

2. Materials and Methods

2.1. Biomass Production

S. salina PCC6906 was cultivated in a 120 L flat panel photobioreactor (FPP) with a light path of 5 cm, 200 cm length and 100 cm height with a total working volume of 100 L. A *S. salina* culture from the Culture Collection of Autotrophic Organisms (CCALA) of the Institute of Botany of the Czech Academy of Sciences was used to inoculate the FPP. The culture was bubbled with a mixture of air and CO₂ (98:2; v/v) at rate of 5 L/min to maintain a high turbulence in the reactor and to prevent the sedimentation of cyanobacterial cells. The FPP surface was illuminated by means of a set of fluorescent lamps TLD 36W/84 (Koninklijke Philips N.V., Amsterdam, The Netherlands) installed on a horizontal

illumination unit. Continuous incident light intensity on the photobioreactor surface was attained by adjusting distance to 80 W/m^2 , measured with a LI-250 light meter (LI-COR Biosciences, Lincoln, NE, USA). The BG-11 medium in semi-batch system was used for cultivation at the constant temperature of $25 \pm 0.5 \text{ }^\circ\text{C}$. After depletion of nitrates from the cultivation medium, the biomass from four-fifths of the total culture volume was harvested by centrifugation at $4000\times g$ and then lyophilized. The remaining one-fifth of the suspension was refilled with freshly prepared BG-11 medium. The cultivation was repeated three times in order to obtain enough freeze-dried *S. salina* biomass. The microalgae growth was monitored as displayed in Figure S1.

2.2. Extract Preparation

For the microalgae extract preparation, an amount of 40 g of dried *S. salina* biomass was extracted with 1 L of 96% (*v/v*) ethanol in an ultrasonic bath for 30 min. The extraction operation was performed in triplicate and the resulting extracts were combined and further centrifuged ($1350\times g$, 10 min) to separate insoluble particles. The solvent was evaporated from the extract in a rotary evaporator under reduced pressure at $38 \text{ }^\circ\text{C}$. The process afforded 4.736 g of dried extract, which was used for the HPCCC isolation of myxoxanthophyll.

2.3. Separation of Myxoxanthophyll Using HPCCC

2.3.1. HPCCC Equipment

For the separation of myxoxanthophyll from *S. salina* extract, a HPCCC equipment, Model Spectrum, (Dynamic Extractions Ltd., Slough, UK) equipped with a separation column of 134 mL (PTFE bore tubing = 3.2 mm) was used. The column rotational speed was controlled with a speed regulator installed into the HPCCC chassis, and the column temperature was maintained at $28 \text{ }^\circ\text{C}$ with a H50/H150 Smart Water Chiller (LabTech Srl, Sorisole Bergamo, Italy). To pump the mobile phase through the column, a Q-Grad pump (LabAlliance, State College, PA, USA) was employed. The chromatographic separation was monitored by a Sapphire UV-VIS detector (ECOM spol. s.r.o., Prague, Czech Republic) at a wavelength of 478 nm. The EZChrom SI software platform (Agilent Technologies, Pleasanton, CA, USA) was used for viewing and recording the chromatogram.

2.3.2. Selection of the Suitable Biphasic Solvent System for HPCCC

Different volume ratios of *n*-heptane, ethanol and water were used for the preparation of several biphasic solvent systems. An ideal solvent system in HPCCC should provide a suitable partition coefficient (*K*) of the target compound [10,15], a short settling time and a proper density difference between the upper and lower phases of the biphasic solvent system [10,15]. For the *K* value determination, a quantity of 2 mg of microalgae extract was dissolved in 2 mL of the pre-equilibrated solvent system composed of 1 mL of each phase. This mixture was shaken well and left for 10 min until the formation of two clear phases. The resulting upper and lower phases were separated and further used for calculating the *K* value by high-performance liquid chromatography with diode array detection (HPLC-DAD). The *K* value was estimated as the ratio between the upper- and lower-phase myxoxanthophyll peak areas. The settling time was measured as previously described [17]. For this purpose, two immiscible phases (2 mL of each phase) of the biphasic solvent system were first equilibrated in a test tube. The capped tube was then gently inverted three times and then immediately placed in an upright position to measure the time required for the two phases to form clear layers with a distinct interface. For measurement of the density difference between the upper and lower phases of each biphasic solvent system, 1 mL of each phase was weighed with a microbalance [15].

2.3.3. HPCCC Separation Process

The separation process was performed using the selected biphasic solvent system composed of *n*-heptane, ethanol, and water. The upper and the lower phases of the resulting biphasic solvent

system were employed as the stationary phase and the mobile phase, respectively. The preparation of the phases for the HPCCC process was performed by mixing the individual solvents in terms of volume ratios. The mixture was vigorously shaken until the creation of two clear immiscible phases. The HPCCC separation process began with filling the column with the stationary phase (upper phase). When the column was full, the HPCCC column was rotated up to 1400 rpm and its temperature was set at 28 °C. Once these two parameters were stable, the pumping of the mobile phase started in order to reach the hydrodynamic equilibrium between the mobile and the stationary phases within the HPCCC column. This occurs when the mobile phase has emerged from the column without the carryover of the stationary phase. At this point, the chromatographic system was ready for the sample injection. The *S. salina* extract dissolved in a volume of the mobile phase served as a sample solution. The HPCCC fractions were manually collected and analyzed by HPLC-DAD.

The retention of the stationary phase (S_f) in the HPCCC column was calculated as follows

$$S_f (\%) = \frac{V_s}{V_c} \times 100 \quad (1)$$

where V_c is the volume of the HPCCC column and V_s is the stationary phase volume in the column when hydrodynamic equilibrium has been achieved [18].

The retention time (t_R) of the target compound in the HPCCC separation was predicted as follows

$$t_R = \frac{V_M + (K \times V_S)}{F} \quad (2)$$

where V_M is the mobile phase volume when the hydrodynamic equilibrium is reached, K is the partition coefficient of the target compound, V_S is the stationary phase volume when the hydrodynamic equilibrium has been reached, and F is the mobile phase flow rate [18].

2.4. Final Purification of the Myxoxanthophyll Fraction by Semi-Preparative HPLC

The myxoxanthophyll fraction obtained from HPCCC was finally purified using a HPLC system (Agilent 1100 Series, Waldbronn, Germany) on a reverse phase semi-preparative column (Eclipse XDB-C8 column, 250 × 9.4 mm, 5 μm) at 30 °C. The combination of water (A) and methanol (B) was used as the mobile phase, which was pumped at a flow rate of 2.5 mL/min in a gradient elution mode that was programmed according to the following conditions: 0–10 min, 70–30% A; 10–35 min, 30–10% A; 35–37 min, 10–0% A; 37–42 min, 0–0% A; 42–45 min, 0–70% A; 45–50 min, 70–70% A. The target compounds in the chromatogram were monitored using a diode array detector (DAD) at 478 nm.

2.5. HPLC-DAD Analysis of Extract and Fractions

The *S. salina* extract and HPCCC fractions were analyzed on an Agilent HPLC system (Agilent 1100 Series, Waldbronn, Germany) equipped with a DAD. The reversed phase column (Luna[®] C8 column, 100 × 4.6 mm, 3 μm) was used for the chromatographic separation at 30 °C, where the mobile phase was composed of the mixture of water (A) and methanol (B), which were constantly pumped at a flow rate of 0.8 mL/min. For the separation, the column was eluted using a linear gradient as follows: 0–20 min, 20–0% A; 20–25 min, 0% A; 25–27 min, 0–20% A; 27–30 min, 20–80% A; 30–35 min, 80% A; 35–42 min, 80–20% A. The HPLC chromatogram was acquired at 478 nm, whereas the absorption spectrum of the target compound was collected from 200 to 700 nm.

2.6. Confirmation of the Chemical Identity of the Purified Target Compound

The chemical identity of the isolated target compound was established using a Dionex UltiMate 3000 HPLC system (Thermo Scientific, Sunnyvale, CA, USA) connected to a high-resolution tandem mass spectrometry (HRMS/MS) detector with electrospray ionization (ESI) source (Impact HD mass spectrometer, Bruker, Billerica, MA, USA) (HPLC-ESI-HRMS/MS). The identification of the target

compound was confirmed in comparison with the published literature data. The conditions for the chromatographic separation are described in Section 2.5. Additionally, a formic acid (0.1%, *v/v*) solution was put in both solvents A and B to achieve a better ionization of the target compound. The operating parameters of the mass spectrometer were established as follows: 4.2 kV of the spray needle voltage, 250 °C of the drying temperature, nitrogen was used as the nebulizing (3 bar) and the drying gas (12 L/min). The scanning range was 50–2000 *m/z* in the positive ion mode with the scanning rate at 2 Hz. For the fragmentation of myxoxanthophyll, the collision energy was set to 35 eV and the collision gas was nitrogen.

2.7. Biological Evaluations

2.7.1. DPPH Free Radical Scavenging Activity

The antioxidant activity of the target compound was determined using 2,2-diphenyl-1-picrylhydrazyl (DPPH) (Sigma-Aldrich, Steinheim, Germany) as a stable free radical. The DPPH assay was performed as described previously [19] with slight modifications. Briefly, 100 µL of the 0.01% (*v/v*) DPPH diluted in methanol was added to 100 µL of the tested substance diluted in methanol with 0.5% (*v/v*) DMSO in a 96-well plate. The absorbance was measured after 30 min at 515 nm using an Envision multimode plate reader (PerkinElmer, Boston, MA, USA). Trolox and astaxanthin (both Sigma-Aldrich, Steinheim, Germany) were used as positive controls.

2.7.2. Inhibition of Tyrosinase Activity

The activity of fungal tyrosinase (2138 U/mL, Sigma-Aldrich, Steinheim, Germany) was measured spectrophotometrically using levodopa (L-DOPA) (Sigma-Aldrich, Steinheim, Germany) as a substrate [20]. A volume of 50 µL of a solution containing the target compound diluted in phosphate buffered saline (PBS) with 8% (*v/v*) DMSO was mixed with 100 µL of L-DOPA (1 mg/mL), 50 µL of fungal tyrosinase (500 U/mL) in PBS and incubated at 37 °C for 30 min. The dopachrome formation was measured at 475 nm using an Envision multimode plate reader (PerkinElmer, Boston, MA, USA). Kojic acid (TCI chemicals, Oxford, United Kingdom) was used as a positive control.

2.7.3. Immune Cell Activation

The immune cell activation was determined by the expression of cell surface glycoprotein CD69 (cluster of differentiation 69), as measured by flow cytometry [21]. Peripheral blood was withdrawn from three healthy volunteers, and further anti-coagulated with sodium heparin. The test sample was prepared at different concentration by dissolving myxoxanthophyll in ex-vivo medium (Bio-Wittaker, Walkersville, MD, USA), which were subsequently filtered through 0.2 µm filters, before use. Phytohemagglutinin (PHA) (Sigma-Aldrich, Steinheim, Germany) was used as a positive control at a concentration of 10 µg/mL. A volume of 100 µL of blood suspension was incubated with 100 µL of test samples into a sterile 96-well flat-bottomed plate at 37 °C with 5% (*v/v*) CO₂ for 24 h. The final concentrations of myxoxanthophyll in the assay media were 20 and 60 µM. After incubation, 10 µL of a cocktail of fluorescently labeled monoclonal antibodies (CD3 PE-Cy5, CD16 PE, CD45 FITC, CD56 PE, and CD69 PE-Cy7) (Immunotech, Marseille, France and Dako, Glostrup, Denmark) was added to the assay media. The phycoerythrin-labeled antibody that is specific to CD69 was used to detect activated immune cells. The antibodies that specifically bind to CD56 and CD16 were used to detect natural killer (NK) cells; antibodies that specifically react with CD45 were used to detect all types of lymphocytes; and antibodies that are specific to CD3 were used to detect T lymphocyte cells. Granulocytes were gated on the basis of their characteristic forward scatter (FSC) and side scatter (SSC) profiles, which represent size and granularity, respectively. The activation of immune cells in response to myxoxanthophyll treatment at 24 h was shown as a shift to the right in the representative histograms. The CD69 expressions on activated cells are shown as mean fluorescent intensity (MFI) values. The activation index (AI), which presents the values of activation, was calculated by dividing

the percentage of activated cells in response to myxoxanthophyll treatment by that of the control. Values higher as $AI \geq 2$ were defined as a positive immune cell response. A Cytomics FC500 flow cytometer (Beckman Coulter, Brea, CA, USA) was used for the analysis, and the obtained data were analyzed by CXP analysis software (Coulter Electronic, Miami, FL, USA). Fluorescence signals from 10,000 events were obtained and presented as logarithmically amplified signals. Every AI value was calculated as the average from three measurements on three different blood samples.

2.8. Statistical Analysis

The one-way Anova test ($p < 0.05$) was applied to determine whether there was a difference among means. Student's *t*-test was used to compare control and test sample at ** $p < 0.01$ and *** $p < 0.001$. A Statistical Package S-Plus 2000 was used for the analysis.

3. Results and Discussion

3.1. Development and Application of the HPCCC Method

In this study, the solvents *n*-heptane, ethanol and distilled water were mixed in different proportions (Table 1) to create several biphasic solvent systems, which were tested for their capacity to be employed in the separation of myxoxanthophyll. First, an adequate biphasic solvent system must provide a proper *K* value ($0.5 \leq K \leq 3$) [15] to allow a good separation of the target compound in HPCCC. Compounds with smaller *K* values are eluted closer to the solvent front showing lower resolution, whereas a larger *K* value gives better resolution, but wider peaks and more dilute peak fractions, because of a later elution time. Second, one of the phases of the suitable biphasic solvent system, which was selected as the stationary phase, should be retained sufficiently within the column to permit the separation process. This latter requirement is met as long as the selected biphasic solvent system has a settling time $t < 30$ s [10] and an appropriate density difference (>0.08 g/mL) between the lower (LP) and upper (UP) phases of the selected biphasic solvent system [15]. As observed in the Table 1, system 7 met those requirements; therefore, it was selected for the HPCCC isolation of myxoxanthophyll. The *K* value (1.517, UP/LP) of the target compound provided by the selected biphasic solvent system (Table 1) indicated a higher affinity of the target compound to the upper phase. This means that if using the upper phase as mobile phase, the target compound would elute closer to the solvent front with a lower resolution. Therefore, in this study, the lower phase of the selected biphasic solvent system was used as the mobile phase, whereas the upper phase was the stationary phase.

Table 1. The partition coefficient (*K*) of myxoxanthophyll in different biphasic solvent systems, density differences and the settling times.

Solvent Systems	Composition	Relative Proportions of Solvents (v/v/v)	Phase Volume Ratio (UP/LP)	Settling Time (s)	Density Difference (LP–UP, g/mL)	Partition Coefficient (<i>K</i>) of MYX
1	<i>n</i> -Hep–EtOH–H ₂ O	5:4:0.5	0.93	8	0.11	0.019
2	<i>n</i> -Hep–EtOH–H ₂ O	5:4:1	1.00	9	0.15	0.025
3	<i>n</i> -Hep–EtOH–H ₂ O	5:4:1.5	0.94	8	0.17	0.045
4	<i>n</i> -Hep–EtOH–H ₂ O	5:4:2	0.96	9	0.19	0.092
5	<i>n</i> -Hep–EtOH–H ₂ O	4:4:2	0.75	16	0.19	0.200
6	<i>n</i> -Hep–EtOH–H ₂ O	3:4:3	0.47	11	0.20	0.736
7	<i>n</i> -Hep–EtOH–H ₂ O	2:4:4	0.30	12	0.22	1.517

LP: Lower phase. UP: Upper phase. MYX: myxoxanthophyll.

The rotational speed of the HPCCC column was established at 1400 rpm. In HPCCC, it is well known that the higher the stationary phase retention inside the column, the better the chromatographic resolution [22]. Sample loading and flow rate are two operational parameters that can positively influence the final yield in HPCCC, however, care must be taken not to overload the sample or increase the flow rate too much, as this can lead to the loss of the stationary phase from the column, which would then be detrimental to the chromatographic resolution [15]. The flow rate of the mobile phase was plotted against the stationary phase retention at a rotational speed of 1400 rpm (Figure 2).

The stationary phase retention was calculated as previously reported [18] using Equation (1) (described in Section 2.3.3). As can be seen in Figure 2, the flow rate of 4 mL/min was selected since it would allow maximum productivity while maintaining 75% of the stationary phase retention within the column. This condition generated a pressure below the maximum level allowed for the column (<250 psi). We observed that 70 mg of biomass extract was the maximum possible amount to be dissolved in 2 mL of stationary phase (2 mL sample loop), since this was its saturation point. Accordingly, 70 mg of sample loading and a flow rate of 4 mL/min were used in this study. Another advantageous aspect of HPCCC is that the retention time of a given target compound can be calculated when the K value and the volume of the stationary phase at the equilibrium are known. In the current study, the retention time of the target compound was estimated as previously established [18] using Equation (2) (described in Section 2.3.3). Therefore, myxoxanthophyll should have a retention time of 46 min. This information is useful in order to estimate a priori the amount of solvent required for the chromatographic process, and it also provides information on the duration of the HPCCC run. As seen in Figure 3, a good separation of myxoxanthophyll was achieved when injecting 70 mg of the sample. In addition, the experimentally determined retention time of the target compound was 40 min (Figure 3), which roughly matches with the previously predicted retention time. This slight discrepancy could occur due to a decrease in the stationary phase retention during the separation process, which may be caused by the sample effect over the hydrodynamic equilibrium.

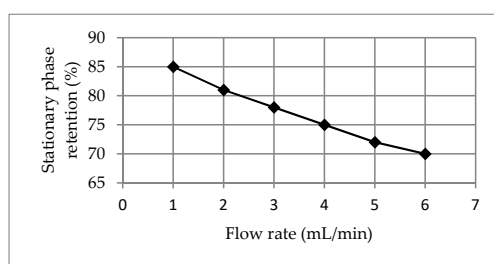


Figure 2. Effect of the mobile phase flow rate over the stationary phase retention. Mobile phase: Lower phase of the biphasic solvent system 7 (*n*-Hep:EtOH:H₂O, 2:4:4, *v/v/v*).

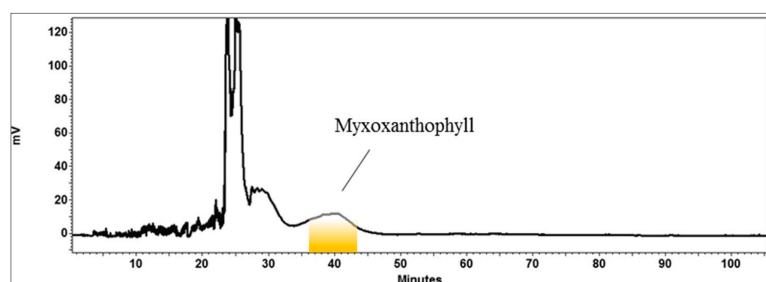


Figure 3. High performance countercurrent chromatography (HPCCC) separation of myxoxanthophyll from *Synechocystis salina* (*S. salina*) extract. Biphasic solvent system: System 7 (*n*-Hep:EtOH:H₂O, 2:4:4, *v/v/v*). Elution mode: Reverse, the mobile phase is the lower phase of the biphasic solvent system 7. Loading per injection: 70 mg of *S. salina* extract. Column rotational speed: 1400 rpm. Flow rate of mobile phase: 4 mL/min. Temperature: 28 °C. Detection: 478 nm.

At this point of the investigation, an efficient HPCCC method to isolate myxoxanthophyll from *S. salina* extract was successfully developed employing the reverse phase elution mode. This means that the lower phase of the selected biphasic solvent system is used as the mobile phase. However, the developed method only involved a single sample injection (70 mg). Accordingly, in order to increase the productivity of the developed method, a multiple-injection system was implemented. In this approach, the hydrodynamic equilibrium needed to obtain the target compound in the first run was re-established without having to stop the rotation of the column to prepare the equipment for a new process. This is achieved using the co-current elution mode, which is performed by simultaneously

pumping the mobile and stationary phases after the myxoxanthophyll elution. Previous investigations have reported the successful application of co-current elution mode using HPCCC to produce lutein [23] and astaxanthins [24] from microalgae. In the current study, the lost volume of stationary phase during the first run (75 mL) was efficiently replenished when pumping stationary and mobile phases at flow rates of 1.5 and 2.5 mL/min, respectively, for 50 min, and shortly after the myxoxanthophyll elution. Consequently, the hydrodynamic equilibrium within the column was newly achieved for a new separation cycle. In conclusion, based on the previously mentioned criteria and conditions, the feasibility of applying a multiple injection HPCCC method to produce myxoxanthophyll from *S. salina* has been demonstrated.

Based on the developed method for obtaining myxoxanthophyll from *S. salina*, the consecutive injections of biomass extract for the continuous production of this pigment were applied. As seen in Figure 4, four consecutive injections were successfully performed when using the previously optimized conditions. An amount of 70 mg of the extract from *S. salina* was injected in each HPCCC run, with each separation cycle lasting 110 min. In total, 280 mg of the *S. salina* extract was processed and yielded 20 mg of myxoxanthophyll with a purity of 95%, as determined by HPLC. The HPLC chromatogram of the isolated compound by HPCCC (Figure 5b) shows the presence of two minor peaks (1 and 2) eluting shortly after the target isolated compound. Accordingly, a final purification step was necessary.

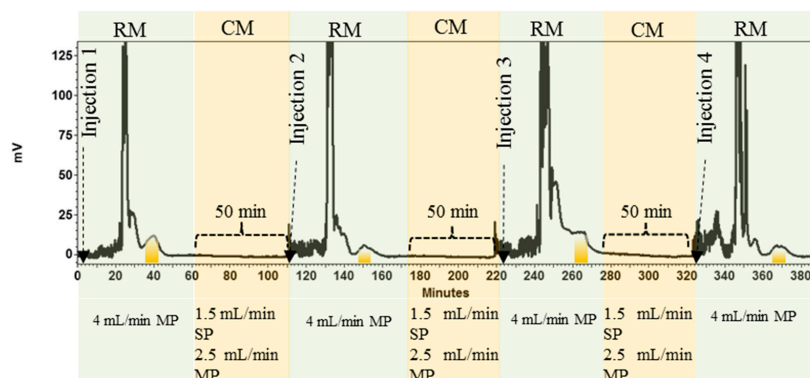


Figure 4. Isolation of myxoxanthophyll by a multi-injection HPCCC method. Biphasic solvent system: System 7 (*n*-Hep:EtOH:H₂O, 2:4:4, *v/v/v*). Elution modes: Reverse (RM) and co-current (CM) elution modes. Loading per injection: 70 mg of *S. salina* extract. Runs: 4 consecutive injections. MP: mobile phase (lower phase of system 7). SP: stationary phase (upper phase of system 7). Rotational speed: 1400 rpm. Column temperature: 28 °C. Detection 478 nm.

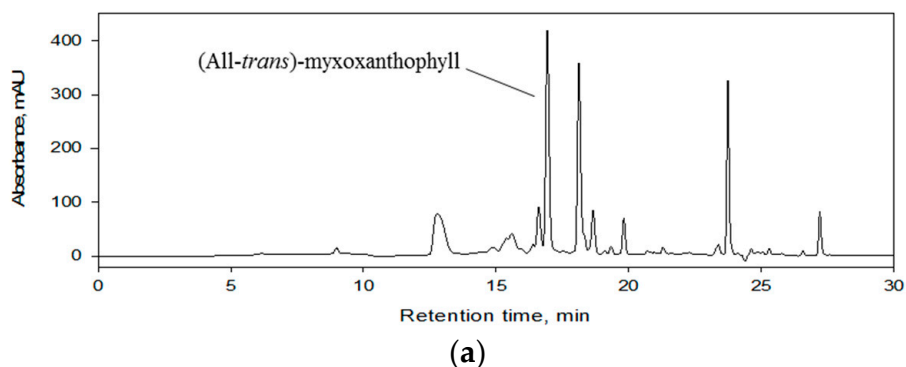


Figure 5. Cont.

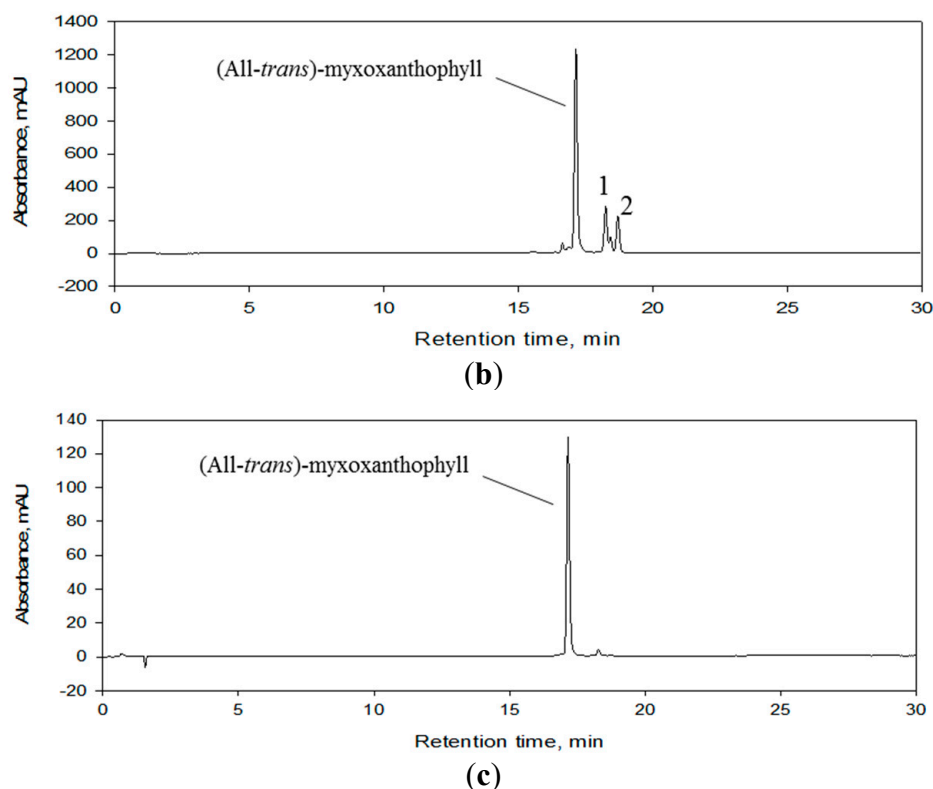


Figure 5. High performance liquid chromatography with diode array detection (HPLC-DAD) chromatograms of *S. salina* extract (a), myxoxanthophyll fraction obtained by HPCCC (b), and myxoxanthophyll further purified by HPLC (c). The chromatograms were monitored at 478 nm. 1: (13 or 13'-cis)- myxoxanthophyll. 2: (9 or 9'-cis)- myxoxanthophyll.

3.2. Final Purification of Myxoxanthophyll Fraction by Semi-Preparative HPLC

The myxoxanthophyll fraction obtained by means of HPCCC was finally purified using semi-preparative HPLC. The resulting compound was dried using a rotary evaporator obtaining 15 mg of myxoxanthophyll and further analyzed by HPLC (Figure 5), demonstrating a purity over 98%. In contrast to previous investigations reporting the isolation of myxoxanthophyll from natural sources [8], this is the first report showing the isolation of this glycosylated carotenoid from *S. salina* using HPCCC. The complementarity and orthogonality of HPCCC and HPLC [15,24] made the separation of this pigment possible.

3.3. Identity Confirmation of the Isolated Target Compound

The identity of the target compound was determined on the basis of its UV-Visible (Figure 6a) and ESI-HRMS (Figure 6c,d) spectra in comparison to the literature data [8]. The ESI-HRMS spectrum of the target compound peak indicated a molecular formula, such as $C_{48}H_{70}O_7$, and a cation radical molecular ion $[M]^+$ at m/z 758.5127 (accuracy -1.4 ppm) (Figure 6c). The ESI-HRMS/MS fragmentation of the cation radical molecular ion gave a fragment ion at m/z 700 (Figure 6d), corresponding to the cleavage of an acetone unit (C_3H_6O) in the cation radical molecular ion, a fragment ion at m/z 525 corresponding to the carotenoid backbone resulting after the cleavage of the sugar moiety, and a fragment ion at m/z 507 formed by the loss of water from the fragment ion at m/z 525, which are in agreement with the fragmentation pattern of (all-trans)- myxoxanthophyll as (3R,2S)-myxol 2'-(2,4-di-O-methyl- α -L-fucoside) [8,25]. The two minor contaminants present in the myxoxanthophyll fraction obtained by means of HPCCC (Figure 5b) exhibited ESI-HRMS/MS spectra similar to those of (all-trans)-myxoxanthophyll, but with UV-Visible spectra that were compatible with those of (13 or 13'-cis)- myxoxanthophyll (1) (Figure 6b) and (9 or 9'-cis)- myxoxanthophyll (2)

(Figure 6b). These two kinds of minor geometrical isomers have been shown to be commonly formed from (all-*trans*)-carotenoids by light and temperature effects, and may not represent any danger to humans [23,26].

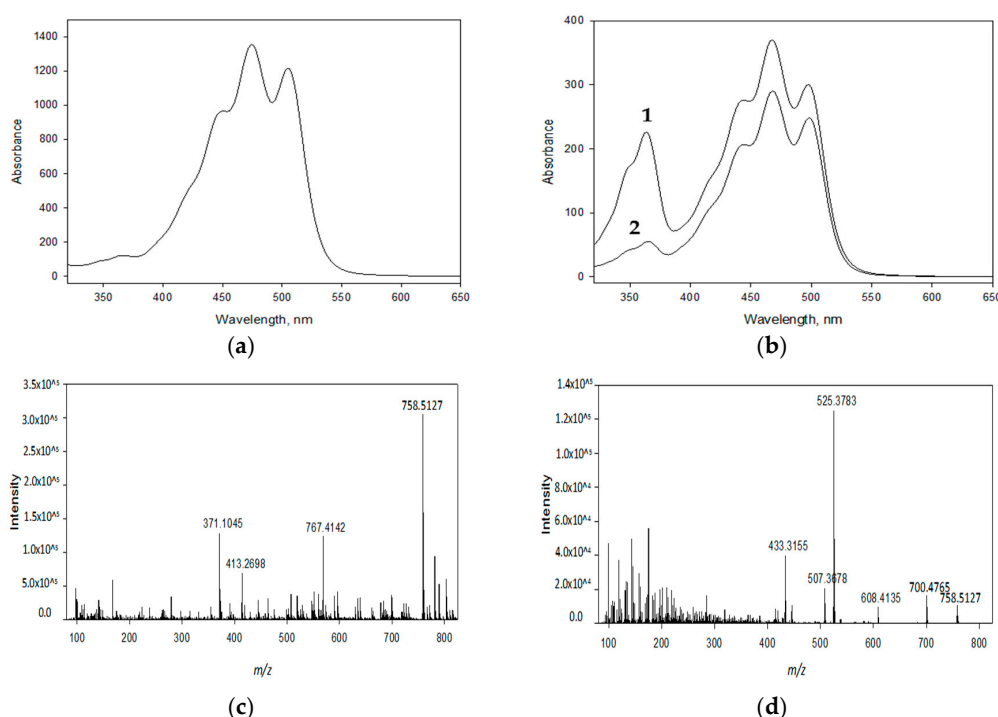


Figure 6. Ultraviolet-visible (UV-Vis) spectra of (all-*trans*)-myxoxanthophyll obtained by HPLC (a). Ultraviolet-visible (UV-Vis) spectra of **1** (13 or 13'-*cis*-myxoxanthophyll) and **2** (9 or 9'-*cis*-myxoxanthophyll) (b). High-resolution mass spectrometry with electrospray ionization (ESI) source (ESI-HR/MS) spectrum of (all-*trans*)-myxoxanthophyll (c). High-resolution tandem mass spectrometry with electrospray ionization source (ESI-HRMS/MS) spectrum of the molecular ion of (all-*trans*)-myxoxanthophyll (d).

3.4. Biological Activity

Recently, there has been a rising interest in exploring the beneficial effects of carotenoids in the healthcare and cosmetic industries [27]. The health benefits of carotenoids are explained by their capacity to scavenge free radicals, which are related to aging and chronic diseases [28]. Epidemiological studies support the observation that adequate carotenoid supplementation may significantly reduce the risk of several disorders mediated by free radicals [29]. On the other hand, melanogenesis is a process to synthesize melanin, which is primarily responsible for the pigmentation of human skin, eye and hair. As tyrosinase plays a major role in melanin synthesis, the inhibition of this enzyme is a common approach in developing anti-melanogenetic agents for skin-whitening cosmetics [30]. In the present study, the capacity of myxoxanthophyll to scavenge the free radical DPPH when compared to the positive controls Trolox and astaxanthin (Figure 7a). As far as the tyrosinase inhibition was concerned, myxoxanthophyll showed a mild inhibiting effect in a concentration non-dependent manner in the concentration range from 10 to 200 μ M (Figure 7b). Although myxoxanthophyll showed only a weak antioxidant and tyrosinase inhibitory effect, its biological effects on other types of free radicals, as well as over other kind of tyrosinase, should still be tested to determine a more comprehensive biological profile of this carotenoid.

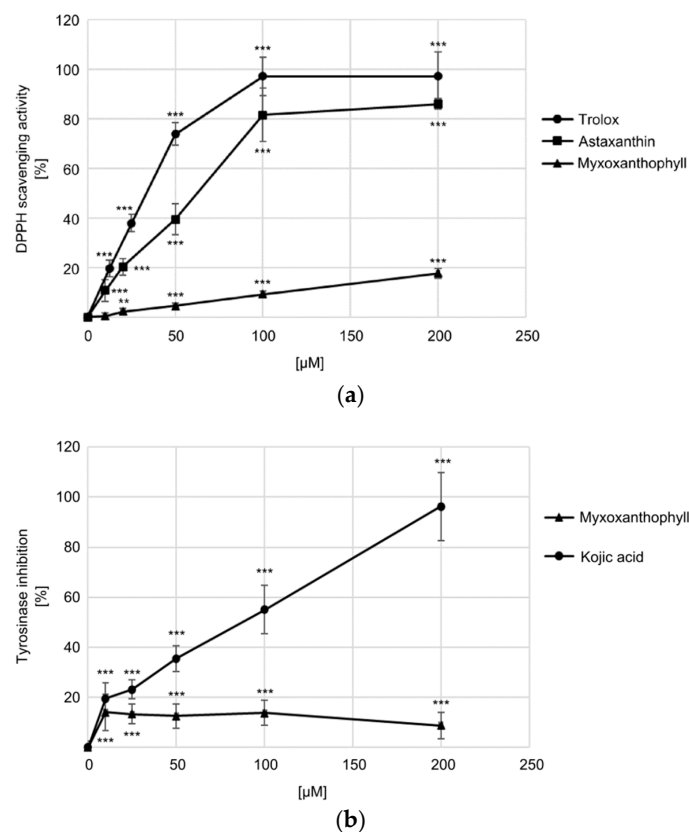


Figure 7. (a) The DPPH (2,2-diphenyl-1-picrylhydrazyl) free radical scavenging activity of the tested substance. Trolox and astaxanthin were used as positive controls. (b) Inhibition of the fungal tyrosinase by myxoxanthophyll using levodopa (L-DOPA) as a substrate. Kojic acid was used as a positive control. The data represent mean±SD. Student’s *t*-test was used for the statistical analysis. ** $p < 0.01$, *** $p < 0.001$ related to control.

The immunomodulating activity of carotenoids such as β -carotene, canthaxanthin and astaxanthin, by improving the proliferation and functions of the immune cell, have been previously reported [31,32]. However, the effect of myxoxanthophyll on the immune system is unknown. In the present study, the potential activation effect on immune cells in response to myxoxanthophyll treatment was investigated, measuring cell surface CD69 expression using flow cytometry. The CD69 glycoprotein is an early activation antigen that is expressed on activated immune cells. Once CD69 is expressed on T lymphocyte cells, it co-stimulates T-cell activation and proliferation. CD69 is also indubitably expressed by B lymphocyte cells, NK cells, monocytes, neutrophils, and eosinophils [33]. This feature has been used to ascertain the immune-stimulating properties of plants using *in vitro* [21,34–37] and *in vivo* studies [38]. As seen in Figure 8, except for granulocytes, no immune cells tested in this investigation were activated by myxoxanthophyll at the concentration range from 20 to 60 μ M. The CD69 expression on activated granulocytes in response to myxoxanthophyll treatment was shown as a shift to the right in the representative histograms (Figure 8c,d). There was an increase in the number of granulocytes in response to myxoxanthophyll treatment, showing a stimulation index of 2.37 and 2.77 when using the target compound at 20 and 60 μ M, respectively. Granulocytes (i.e., neutrophils, eosinophils, basophils, and mast cells) are effector cells of the innate immune response against bacterial and fungal infections. These cells identify, ingest and destroy microbial pathogens through receptors, oxidative mechanisms, and enzymes including lysozyme, collagenase, and elastase [39]. The data presented in this study may support the potential utilization of myxoxanthophyll for strengthening the immune system against bacterial and fungal infections.

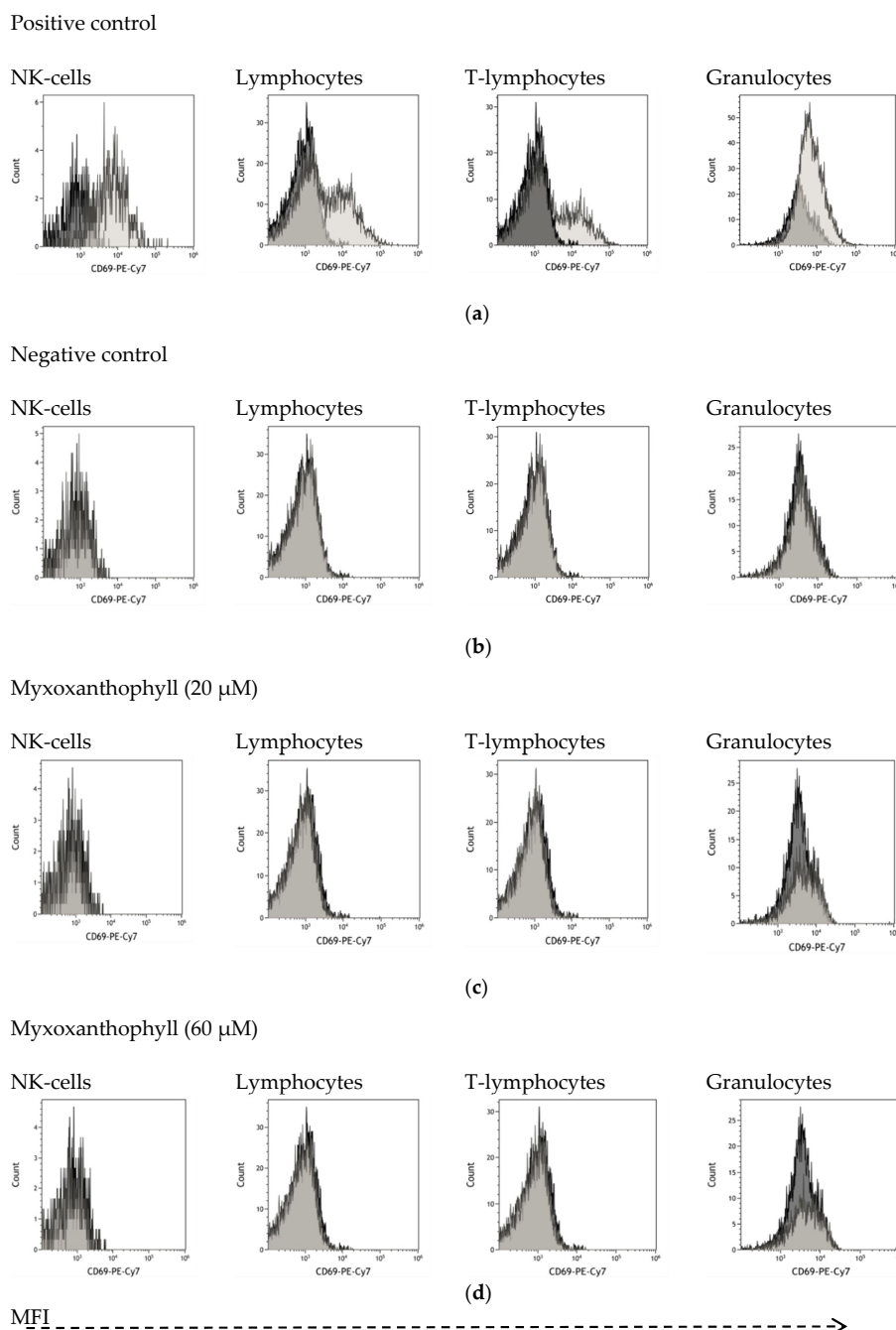


Figure 8. Mean fluorescent intensity (MFI) of CD69 expression on activated immune cells from human peripheral blood in response to treatment with myxoxanthophyll for 24 h is shown as histograms. The filled histograms (dark grey) represent the group control (untreated) and the other histograms (light grey) the stimulated (pretreated) group. The mitogen phytohemagglutinin (PHA) was used as a positive control, showing the activation of immune cells (a). In negative control, the cells were treated neither with myxoxanthophyll nor PHA, and no immune cell activation was observed (b). Granulocytes were activated by myxoxanthophyll at 20 μ M (c) and 60 μ M (d). The histograms are representative of three separate experiments using cells from three different healthy donors.

4. Conclusions

Most efforts aimed at obtaining pigments from microalgae have been addressed separately, either at the level of biomass production or extraction operations. The current study presents an isolation approach based on a sequential separation HPLC process integrated to autotrophic cultivation of

the cyanobacterium *S. salina* for obtaining myxoxanthophyll. Compared to the multi-step procedures used to date to obtain this compound, the present approach uses only a single type of separation technique. As the target compound obtained in this process has potential applications in the food or nutraceutical sectors, the evaporation and drying operations involved in this process ensured that no residual solvent remained in the final product. This pigment could have applications as a potential nonspecific immune stimulator. Overall, the developed HPCCC method represents a good strategy to efficiently isolate myxoxanthophyll from the cyanobacterium *S. salina* and can serve as a reference for developing a large-scale production model of cyanobacteria-based myxoxanthophyll. In comparison to liquid–solid chromatography where a solid stationary phase is used, no expensive columns are required in countercurrent chromatography. Therefore, the use of HPCCC for the large-scale production of myxoxanthophyll is foreseen to lead to significant cost savings. In future, this strategy may converge towards a bio-refinery approach with potential for expansion and diversification in terms of other valuable co-products.

Supplementary Materials: The following are available online at <http://www.mdpi.com/2297-8739/7/4/73/s1>, Figure S1: Growth curve of *S. salina* in 120 L flat panel photobioreactor.

Author Contributions: Conceptualization, J.C.; methodology, J.C., M.N. and T.F.; formal analysis, D.V., I.D., J.K., L.T. and P.H.; investigation, M.N., T.F. and J.C.; writing—original draft preparation, J.C.; writing—review and editing, J.C., M.N., T.F. and P.H.; supervision, J.C. Both authors (M.N. and T.F.) contributed equally to this manuscript, and share co-first authorship. All authors have read and agreed to the published version of the manuscript.

Funding: This research was funded by the National Programme of Sustainability I of the The Ministry of Education, Youth and Sports of the Czech Republic, grant number ID: LO1416.

Acknowledgments: Michaela Nováková and Tereza Fábryová gratefully acknowledge the scientific supervision of José Cheel (Centre Algatech—Czech Academy of Sciences) during the postgraduate study.

Conflicts of Interest: The authors declare no conflict of interest.

References

1. Yu, Y.; You, L.; Liu, D.; Hollinshead, W.; Tang, Y.J.; Zhang, F. Development of *Synechocystis* sp. PCC 6803 as a phototrophic cell factory. *Mar. Drugs* **2013**, *11*, 2894–2916. [[CrossRef](#)] [[PubMed](#)]
2. Saini, D.K.; Pabbi, S.; Shukla, P. Cyanobacterial pigments: Perspectives and biotechnological approaches. *Food Chem. Toxicol.* **2018**, *120*, 616–624. [[CrossRef](#)] [[PubMed](#)]
3. Mohamed, H.E.; van de Meene, A.M.L.; Roberson, R.W.; Vermaas, W.F.J. Myxoxanthophyll is required for normal cell wall structure and thylakoid organization in the cyanobacterium *Synechocystis* sp. strain PCC 6803. *J. Bacteriol.* **2005**, *187*, 6883–6892. [[CrossRef](#)] [[PubMed](#)]
4. Shindo, K.; Kikuta, K.; Suzuki, A.; Katsuta, A.; Kasai, H.; Yasumoto-Hirose, M.; Matsuo, Y.; Misawa, N.; Takaichi, S. Rare carotenoids, (3R)-saproxanthin and (3R,2'S)-myxol, isolated from novel marine bacteria (Flavobacteriaceae) and their antioxidative activities. *Appl. Microbiol. Biotechnol.* **2007**, *74*, 1350–1357. [[CrossRef](#)]
5. Ghosh, T.; Bhayani, K.; Paliwal, C.; Maurya, R.; Chokshi, K.; Pancha, I.; Mishra, S. Cyanobacterial pigments as natural anti-hyperglycemic agents: An *in vitro* study. *Front. Mar. Sci.* **2016**, *3*, 146. [[CrossRef](#)]
6. Steiger, S.; Schäfer, L.; Sandmann, G. High-light-dependent upregulation of carotenoids and their antioxidative properties in the cyanobacterium *Synechocystis* PCC 6803. *J. Photochem. Photobiol. B Biol.* **1999**, *52*, 14–18. [[CrossRef](#)]
7. Jaeger, C.; Saettler, A.; Schroeder, K.R.; Roegner, M. Use of Myxoxanthophyll and/or Echinenon for the Prophylactic and/or Therapeutic Treatment of Undesirable Physical Conditions Caused or Promoted by Oxidative Processes. Patent DE10046838A1, Germany. 2000. Available online: <https://patents.google.com/patent/DE10046838A1/en> (accessed on 15 October 2020).
8. Takaichi, S.; Maoka, T.; Masamoto, K. Myxoxanthophyll in *Synechocystis* sp. PCC 6803 is myxol 2'-dimethyl-fucoside, (3R,2'S)-myxol 2'-(2,4-di-O-methyl- α -L-fucoside), not rhamnocide. *Plant Cell Physiol.* **2001**, *42*, 756–762. [[CrossRef](#)]

9. Sutherland, I.; Thickitt, C.; Douillet, N.; Freebairn, K.; Johns, D.; Mountain, C.; Wood, P.; Edwards, N.; Rooke, D.; Harris, G.; et al. Scalable technology for the extraction of pharmaceuticals: Outcomes from a 3 year collaborative industry/academia research programme. *J. Chromatogr. A* **2013**, *1282*, 84–94. [[CrossRef](#)]
10. Ito, Y. Golden rules and pitfalls in selecting optimum conditions for high-speed counter-current chromatography. *J. Chromatogr. A* **2005**, *1065*, 145–168. [[CrossRef](#)]
11. Michel, T.; Destandau, E.; Elfakir, C. New advances in countercurrent chromatography and centrifugal partition chromatography: Focus on coupling strategy. *Anal. Bioanal. Chem.* **2014**, *406*, 957–969. [[CrossRef](#)]
12. Chen, F.; Li, H.B.; Wong, R.; Ji, B.; Jiang, Y. Isolation and purification of the bioactive carotenoid zeaxanthin from the microalga *Microcystis aeruginosa* by high-speed counter-current chromatography. *J. Chromatogr. A* **2005**, *1064*, 183–186. [[CrossRef](#)] [[PubMed](#)]
13. Chen, T.; Liu, Y.; Zou, D.; Chen, C.; You, J.; Zhou, G.; Sun, J.; Li, Y. Application of an efficient strategy based on liquid–liquid extraction, high-speed counter-current chromatography, and preparative HPLC for the rapid enrichment, separation, and purification of four anthraquinones from *Rheum tanguticum*. *J. Sep. Sci.* **2014**, *37*, 165–170. [[CrossRef](#)] [[PubMed](#)]
14. Zhang, L.; Yue, H.L.; Zhao, X.H.; Li, J.; Shao, Y. Separation of four phenylpropanoid glycosides from a chinese herb by HSCCC. *J. Chromatogr. Sci.* **2015**, *53*, 860–865. [[CrossRef](#)] [[PubMed](#)]
15. Cheel, J.; Urajová, P.; Hájek, J.; Hrouzek, P.; Kuzma, M.; Bouju, E.; Faure, K.; Kopecký, J. Separation of cyclic lipopeptide puwainaphycins from cyanobacteria by countercurrent chromatography combined with polymeric resins and HPLC. *Anal. Bioanal. Chem.* **2017**, *409*, 917–930. [[CrossRef](#)]
16. Cheel, J.; Hájek, J.; Kuzma, M.; Saurav, K.; Smýkalová, I.; Ondráčková, E.; Urajová, P.; Vu, D.L.; Faure, K.; Kopecký, J.; et al. Application of HPCCC combined with polymeric resins and HPLC for the separation of cyclic lipopeptides muscotoxins A–C and their antimicrobial activity. *Molecules* **2018**, *23*, 2653. [[CrossRef](#)] [[PubMed](#)]
17. Ito, Y.; Conway, W.D. Experimental observations of the hydrodynamic behavior of solvent systems in high-speed counter-current chromatography. III. Effects of physical properties of the solvent systems and operating temperature on the distribution of two-phase solvent systems. *J. Chromatogr. A* **1984**, *301*, 405–414. [[CrossRef](#)]
18. Sutherland, I.A. Liquid stationary phase retention and resolution in hydrodynamic CCC. In *Comprehensive Analytical Chemistry*; Berthod, A., Ed.; Elsevier Science B.V.: Amsterdam, The Netherlands, 2002; Volume 38, pp. 159–176. [[CrossRef](#)]
19. Brand-Williams, W.; Cuvelier, M.E.; Berset, C. Use of a free radical method to evaluate antioxidant activity. *LWT* **1995**, *28*, 25–30. [[CrossRef](#)]
20. Jiménez, M.; Chazarra, S.; Escribano, J.; Cabanes, J.; García-Carmona, F. Competitive inhibition of mushroom tyrosinase by 4-substituted benzaldehydes. *J. Agric. Food Chem.* **2001**, *49*, 4060–4063. [[CrossRef](#)]
21. Tůmová, L.; Dučaiová, Z.; Cheel, J.; Vokřál, I.; Sepúlveda, B.; Vokurková, D. Azorella compacta infusion activates human immune cells and scavenges free radicals in vitro. *Pharmacogn. Mag.* **2017**, *13*, 260–264. [[CrossRef](#)]
22. Berthod, A.; Faure, K. Separations with a liquid stationary phase: Countercurrent chromatography or centrifugal partition chromatography. In *Analytical Separation Science*, 1st ed.; Anderson, J.L., Berthod, A., Pino Estévez, V., Stalcup, A.M., Eds.; Wiley-VCH Verlag GmbH & Co. KGaA: Weinheim, Germany, 2015; pp. 1177–1206. [[CrossRef](#)]
23. Fábryová, T.; Cheel, J.; Kubáč, D.; Hrouzek, P.; Vu, D.L.; Tůmová, L.; Kopecký, J. Purification of lutein from the green microalgae *Chlorella vulgaris* by integrated use of a new extraction protocol and a multi-injection high performance counter-current chromatography (HPCCC). *Algal Res.* **2019**, *41*, 101574. [[CrossRef](#)]
24. Fábryová, T.; Tůmová, L.; da Silva, D.C.; Pereira, D.M.; Andrade, P.B.; Valentão, P.; Hrouzek, P.; Kopecký, J.; Cheel, J. Isolation of astaxanthin monoesters from the microalgae *Haematococcus pluvialis* by high performance countercurrent chromatography (HPCCC) combined with high performance liquid chromatography (HPLC). *Algal Res.* **2020**, *49*, 101947. [[CrossRef](#)]
25. Lagarde, D.; Vermaas, W. The zeaxanthin biosynthesis enzyme IS-carotene hydroxylase is involved in myxoxanthophyll synthesis in *Synechocystis* sp. PCC 6803. *FEBS Lett.* **1999**, *454*, 247–251. [[CrossRef](#)] [[PubMed](#)]

26. Aman, R.; Schieber, A.; Carle, R.J. Effects of heating and illumination on trans-cis isomerization and degradation of *beta*-carotene and lutein in isolated spinach chloroplasts. *J. Agric. Food Chem.* **2005**, *53*, 9512–9518. [CrossRef] [PubMed]
27. Sathasivam, R.; Ki, J.S. A Review of the biological activities of microalgal carotenoids and their potential use in healthcare and cosmetic industries. *Mar. Drugs* **2018**, *16*, 26. [CrossRef] [PubMed]
28. Halliwell, B.; Gutteridge, J.M. Oxygen toxicity, oxygen radicals, transition metals and disease. *Biochem. J.* **1984**, *219*, 1–14. [CrossRef]
29. Fiedor, J.; Burda, K. Potential role of carotenoids as antioxidants in human health and disease. *Nutrients* **2014**, *6*, 466–488. [CrossRef]
30. Pillaiyar, T.; Manickam, M.; Namasivayam, V. Skin whitening agents: Medicinal chemistry perspective of tyrosinase inhibitors. *J. Enzym. Inhib. Med. Chem.* **2017**, *32*, 403–425. [CrossRef]
31. Okai, Y.; Higashi-Okai, K. Possible immunomodulating activities of carotenoids in *in vitro* cell culture experiments. *Int. J. Immunopharmacol.* **1996**, *18*, 753–758. [CrossRef]
32. Hughes, D.A. Effects of carotenoids on human immune function. *Proc. Nutr. Soc.* **1999**, *58*, 713–718. [CrossRef]
33. Ziegler, S.F.; Ramsdell, F.; Alderson, M.R. The activation antigen CD69. *Stem Cells* **1994**, *12*, 456–465. [CrossRef]
34. Cheel, J.; Antwerpen, P.V.; Tůmová, L.; Onofre, G.; Vokurková, D.; Zouaoui-Boudjeltia, K.; Vanhaeverbeek, M.; Nève, J. Free radical-scavenging, antioxidant and immunostimulating effects of a licorice infusion (*Glycyrrhiza glabra* L.). *Food Chem.* **2010**, *122*, 508–517. [CrossRef]
35. Cheel, J.; Onofre, G.; Vokurková, D.; Tůmová, L.; Neugebauerová, J. Licorice infusion: Chemical profile and effects on the activation and the cell cycle progression of human lymphocytes. *Pharmacogn. Mag.* **2010**, *6*, 26–33. [CrossRef] [PubMed]
36. Wagner, H.; Jurcic, K. Immunological studies of Revitonil[®], a phytopharmaceutical containing *Echinacea purpurea* and *Glycyrrhiza glabra* root extract. *Phytomedicine* **2002**, *9*, 390–397. [CrossRef] [PubMed]
37. Zwickey, H.; Brush, J.; Iacullo, C.M.; Connelly, E.; Gregory, W.L.; Soumyanath, A.; Buresh, R. The effect of *Echinacea purpurea*, *Astragalus membranaceus* and *Glycyrrhiza glabra* on CD25 expression in humans: A pilot study. *Phytother. Res.* **2007**, *21*, 1109–1112. [CrossRef] [PubMed]
38. Brush, J.; Mendenhall, E.; Guggenheim, A.; Chan, T.; Connelly, E.; Soumyanath, A.; Buresh, R.; Barrett, R.; Zwickey, H. The effect of *Echinacea purpurea*, *Astragalus membranaceus* and *Glycyrrhiza glabra* on CD69 expression and immune cell activation in humans. *Phytother. Res.* **2006**, *20*, 687–695. [CrossRef] [PubMed]
39. Aristizábal, B.; González, Á. Innate immune system. In *Autoimmunity: From Bench to Bedside*; Anaya, J.M., Shoenfeld, Y., Rojas-Villarraga, A., Levy, R.A., Cervera, R., Eds.; El Rosario University Press: Bogota, Colombia, 2013; pp. 31–46. Available online: <https://www.ncbi.nlm.nih.gov/books/NBK459455/> (accessed on 15 October 2020).

Publisher’s Note: MDPI stays neutral with regard to jurisdictional claims in published maps and institutional affiliations.



© 2020 by the authors. Licensee MDPI, Basel, Switzerland. This article is an open access article distributed under the terms and conditions of the Creative Commons Attribution (CC BY) license (<http://creativecommons.org/licenses/by/4.0/>).